Geometric and electronic structure of Sb on Si(111) by scanning tunneling microscopy

H. B. Elswijk, D. Dijkkamp, and E. J. van Loenen
Philips Research Laboratories, P.O. Box 80 000, 5600 JA Eindhoven, The Netherlands
(Received 28 January 1991)

Scanning tunneling microscopy and spectroscopy (STS) are used to investigate the Si(111)-Sb surface. At an Sb coverage of a few percent of a monolayer (ML), Sb substitutes Si adatoms in the 7×7 reconstruction. At about $\frac{1}{3}$ ML, the 7×7, "disordered 7×7," and $\sqrt{3}\times\sqrt{3}$-$R30°$ reconstructions are observed. This sub-ML $\sqrt{3}\times\sqrt{3}$ reconstruction is a simple adatom phase. The $T4$ site is identified as the chemical bonding site of Sb adatoms in these low-coverage reconstructions. Spatially resolved STS shows the complex nature of the electronic structure of Si(111)7×7-Sb as compared to the clean Si surface. At the saturation coverage of 1 ML, domains of 1×1, 2×1, and a different $\sqrt{3}\times\sqrt{3}$ reconstruction are observed, and structure models are proposed.

I. INTRODUCTION

The importance of group-V elements such as Sb and As as dopants in semiconductor technology has prompted interest in their interaction with Si and Ge crystal surfaces in recent years. Sb and As are known to segregate strongly during epitaxial crystal growth. This phenomenon hinders the formation of sharply controlled doping profiles in molecular-beam epitaxy, but on the other hand may be employed beneficially to manipulate surface energetics and mediate growth of heteroepitaxial structures of Si-Ge.[1]

The atomic structure of the As-terminated Si(111) surface has been thoroughly studied and is well understood.[2–5] It forms a 1×1 surface structure at one-monolayer (ML) coverage and passivates the surface by saturating the Si dangling bonds. The Sb-terminated Si(111) surface exhibits a more complex behavior: A diversity of Sb-induced reconstructions has been observed with low-energy electron diffraction (LEED) including 1×1, 2×2 (or three-domain 2×1), $\sqrt{3}\times\sqrt{3}$-$R30°$ (simply $\sqrt{3}\times\sqrt{3}$ below), $5\sqrt{3}\times5\sqrt{3}$-$R30°$ ($5\sqrt{3}\times5\sqrt{3}$), $7\sqrt{3}\times7\sqrt{3}$-$R30°$ ($7\sqrt{3}\times7\sqrt{3}$), and 7×7.[6] We use scanning tunneling microscopy (STM) and scanning tunneling spectroscopy (STS) in order to investigate the real-space structure of the Si(111)-Sb surface at various coverages.

II. EXPERIMENT

The vicinal Si(111) sample used in this study ($20\times5\times0.3$ mm^3) is cut from a commercially available wafer (Monsanto, 7–21 Ω cm, p-type, B doped). The sample has a misorientation of 3.8° in the $[11\bar{2}]$ direction, as determined by x-ray diffraction. After rinsing in pure ethanol, the sample is inserted into the microscope ultrahigh-vacuum (UHV) chamber (base pressure 10^{-10} Torr) and kept at a temperature of 900 K overnight to degas sample and holder. Before the experiments, it is flashed to about 1520 K for 1 min to remove oxide and carbides from the surface. After flashing, cooling to 1000 K is performed at a rate of 25 K/min, followed by quenching to room temperature, resulting in a surface with large (111) 7×7 terraces, separated by bunches of atomic steps with an average height of about 14 atomic layers, as observed by STM before Sb deposition.

Subsequently, Sb is deposited from an effusion cell at a cell temperature of 670 K, resulting in a flux of about 10^{13} atoms/cm^2 s at the sample position, as calibrated by Rutherford backscattering spectrometry. The conditions to prepare the various surface reconstructions are taken from Ref. 6. After preparation of a surface, the sample is allowed to cool to room temperature to reduce thermal drift. Constant-current topographs are recorded at various bias voltages to obtain information on both occupied and unoccupied electronic states. In order to provide density-of-states (DOS) information, STS is performed. In this technique, current-voltage curves are measured simultaneously with the topography. The acquired I-V data give information about the surface DOS, as has been demonstrated previously.[7]

III. RESULTS AND DISCUSSION

A. Sub-ML coverage

1. *Surface structure*

Figure 1 shows the surface geometry after the deposition of a few percent of a ML of Sb at 900 K, and a subsequent anneal of 2 min at 900 K (the substrate temperature is measured with an optical pyrometer with an accuracy of 50 K). The LEED study showed a diffuse 7×7 pattern under these conditions.[6] The sample bias with respect to the PtIr probe tip is -2.5 V; hence tunneling occurs from the occupied states of the sample. The 7×7 reconstruction is still the dominant surface structure. However, the deposited Sb has induced a variety of features on the surface. First, different levels of apparent brightness of the adatoms in the 7×7 reconstruction can be distinguished: There are "bright" and "dim" adatoms. On the average about 1 of every 12 adatoms in a unit cell is bright. Second, clusters or islands of the size

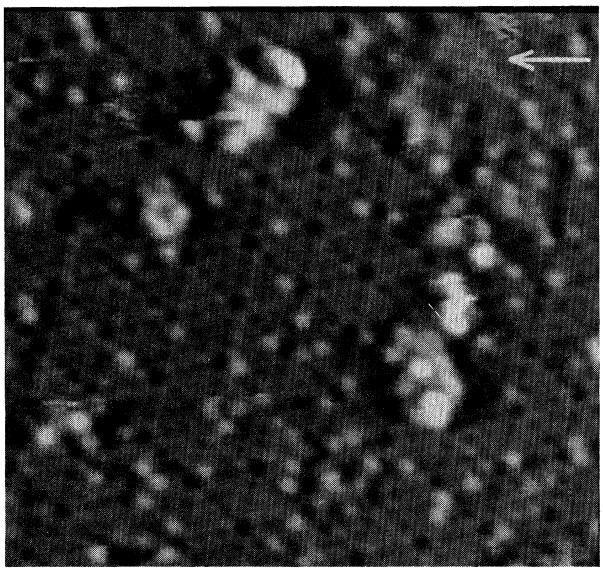

FIG. 1. STM image of 24×20-nm^2 Si(111) 7×7 area after deposition of about 0.03 ML of Sb and an anneal of 2 min at 900 ± 50 K. $V_{\text{sample}}=-2.5$ V, $I=0.5$ nA. Brightly imaged adatoms and clusters and a nucleus of the $\sqrt{3}\times\sqrt{3}$ reconstruction (arrow) can be seen.

of one to two 7×7 unit cells are observed, and third, small nuclei of a different reconstruction are present (one such nucleus is indicated by the arrow in Fig. 1).

First, the contrast difference between adatoms will be discussed. In a gray-scale constant-current STM image such as Fig. 1, the brightness reflects the vertical position (z) of the probe, as it is scanned over the surface (x,y) at constant tunneling current. Since the tunneling current is a sensitive function of both the distance from tip to surface and of the electronic structure of the sample, the resulting image is a convolution of geometric and electronic structure. We find that at a sample bias of -2.5 V, the trace of the probe tip over the brightly imaged adatoms protrudes 0.06 nm with respect to its trace over the dim ones. On inverting the bias voltage to $+2.0$ V, the contrast difference inverts and the adatoms appearing as protrusions at negative-bias voltage, now appear to be depressed (again, by about 0.06 nm) with respect to the others. The contrast difference is therefore mostly electronic rather than geometric in this case. The interpretation of these observations is straightforward: deposited Sb atoms can replace Si adatoms in the 7×7 reconstruction. Since Sb has five valence electrons, it will form three bonds with three Si atoms in the second layer and have a lone-pair orbital protruding into the vacuum. Qualitatively, it is then understandable that Sb shows up more brightly than Si while tunneling from filled states, and Si images more brightly while tunneling into the empty dangling-bond (DB) state. Similar STM observations have been reported for small coverages of the group-III elements Ga and In on Si(111) 7×7, where the adsorbate adatoms imaged more brightly than Si adatoms at a positive sample voltage.[8,9]

The observed clusters are possibly formed from displaced Si atoms or, alternatively, from clustered Sb and are probably responsible for the diffuse background in LEED as reported in Ref. 6. The surface structure observed in the small nucleus indicated by the arrow in Fig. 1 has the orientation and periodicity of a $\frac{1}{3}$-ML $\sqrt{3}\times\sqrt{3}$ adatom reconstruction and will be discussed below.

Figures 2(a), 3, and 4(a) show the surface after deposition of a few tenths of a ML of Sb at the substrate temperature of 900 K and after an anneal of 1 min at 1000 K. According to the LEED study, a mixture of 7×7, disordered 7×7, $5\sqrt{3}\times5\sqrt{3}$, and $7\sqrt{3}\times7\sqrt{3}$ reconstructed areas are present under these conditions. In real space we find three different surface reconstructions to coexist: the 7×7, $\sqrt{3}\times\sqrt{3}$, and "disordered 7×7."

In Fig. 2(a) a phase boundary is seen between the 7×7 and $\sqrt{3}\times\sqrt{3}$ reconstructions. The density of bright spots in the 7×7 area is larger than in Fig. 1 because the

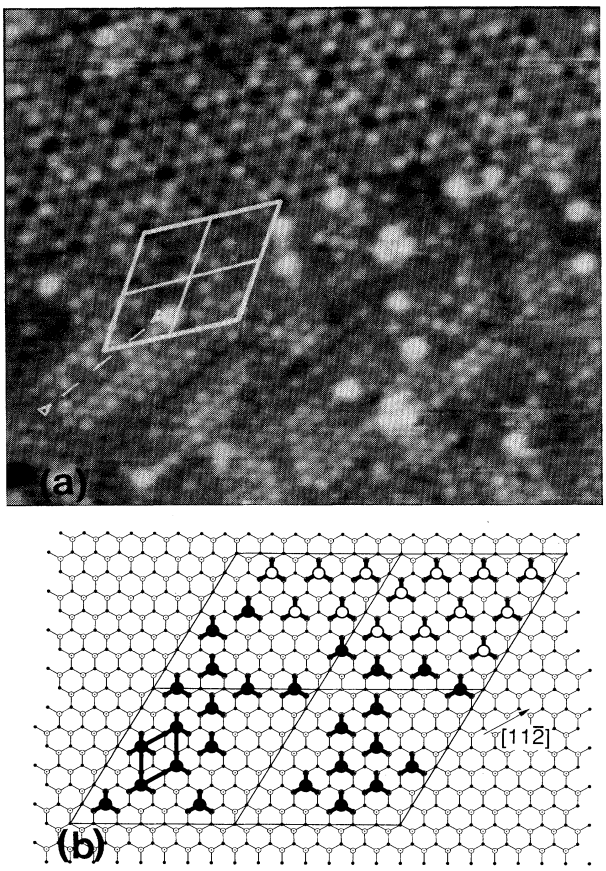

FIG. 2. (a) STM image of 25×22-nm^2 Si(111) surface with about 0.3 ML of Sb, after 2-min anneal at 1000 ± 50 K. $V_{\text{sample}}=-2.5$ V, $I=0.5$ nA. A phase boundary between the 7×7 and $\frac{1}{3}$-ML $\sqrt{3}\times\sqrt{3}$ reconstruction is observed. The area in the rhombus is mapped in (b). The dashed line between the arrows indicates an antiphase boundary within the $\sqrt{3}\times\sqrt{3}$ area. (b) Schematic representation of the adatom positions in the 7×7 and $\frac{1}{3}$-ML $\sqrt{3}\times\sqrt{3}$ reconstructions as seen in (a); a $\sqrt{3}\times\sqrt{3}$ cell is indicated. Open symbols denote adatoms in the 7×7 reconstruction; solid symbols denote adatoms in the $\sqrt{3}\times\sqrt{3}$ reconstruction. All adatoms are located on $T4$ sites. Stacking faults and dimers which are present in the 7×7 reconstruction are omitted.

Sb coverage is higher. Also, there is a range of levels of brightness of adatoms in contrast to the two discrete levels in Fig. 1. This can be understood as follows: At the low coverage in Fig. 1, the Sb concentration is such that the Sb adatoms can be regarded as isolated defects. At the present coverage of roughly 30% of a ML, the local environment of the adatoms consists of a mixture of Si and Sb atoms. The varying local configuration will give rise to a varying local density of states at the tunneling bias and a range of levels of brightness in the STM image. Consequently, it is now impossible to clearly distinguish Sb and Si adatoms. The variation in the local electronic structure will be discussed in more detail in the following section.

From Fig. 2(a) a slight preference for substitution of adatoms in the faulted half of the 7×7 unit cell is observed: 65% of the bright adatoms are found in the faulted half. Assuming the observed distribution to be in local thermodynamical equilibrium at 1000 K, a difference in binding energy between the two halves can be estimated: $\Delta E = 0.05 \pm 0.02$ eV. The preference for disruption of the faulted half of the unit cell has also been observed for other metals on Si(111) 7×7.[10–12] No difference in occupancy between adatom sites adjacent to corner holes and those not adjacent to corner holes is observed.

The phase in the lower part of Fig. 2(a) can be interpreted as a simple $\frac{1}{3}$-ML $\sqrt{3}\times\sqrt{3}$ adatom phase. Each adatom saturates three dangling bonds, and at a coverage of $\frac{1}{3}$ ML all dangling bonds are saturated. The examination of the phase boundary in Fig. 2(a) between the 7×7 and $\frac{1}{3}$-ML $\sqrt{3}\times\sqrt{3}$ reconstructions offers the opportunity to determine the bonding site of the $\frac{1}{3}$-ML $\sqrt{3}\times\sqrt{3}$ adatoms by directly measuring their registry with the underlying Si lattice. The most appropriate procedure to determine the $\frac{1}{3}$-ML $\sqrt{3}\times\sqrt{3}$ adatom site in this case is the extrapolation of lines through rows of these sites in the $[\bar{1}2\bar{1}]$ and $[11\bar{2}]$ directions. The location of the intersection of these lines gives the type of bonding site of the $\frac{1}{3}$-ML $\sqrt{3}\times\sqrt{3}$ adatoms and can be measured with great precision in the 7×7 reconstruction.

The $\frac{1}{3}$-ML $\sqrt{3}\times\sqrt{3}$ adatoms are found to be positioned on $T4$ bonding sites, on top of second-layer Si atoms. The $T4$ site has been shown to be a favorable bonding site for other adsorbates such as Sn, Ga, In, and Al.[5,10–15] Figure 2(b) schematically shows the registry of the 7×7 and $\frac{1}{3}$-ML $\sqrt{3}\times\sqrt{3}$ adatoms in the rhombus indicated in Fig. 2(a). From the appearance of the $\frac{1}{3}$-ML $\sqrt{3}\times\sqrt{3}$ adatom image spots, it is concluded that a single atom is imaged rather than a triplet, as has been proposed to be present in the milk-stool model of the 1-ML $\sqrt{3}\times\sqrt{3}$ Sb- or Bi-induced reconstruction.[16–18] It will

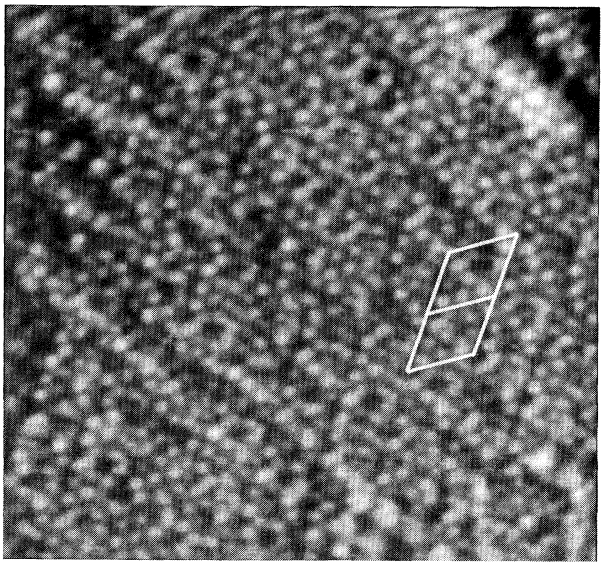

FIG. 3. STM image at a sample bias of -2.5 V, $I=0.5$ nA, and 24×24 nm^2. A 2D fast Fourier transform shows the 7×7 periodicity, but the real-space structure is highly disordered. Two 7×7 cells are indicated. Corner holes are recognizable and often contain a protrusion in the center. The adatoms in the faulted half (upper-right half) of the unit cells are located on random $T4$ sites, while in the unfaulted half most are at the correct position in the 7×7 reconstruction.

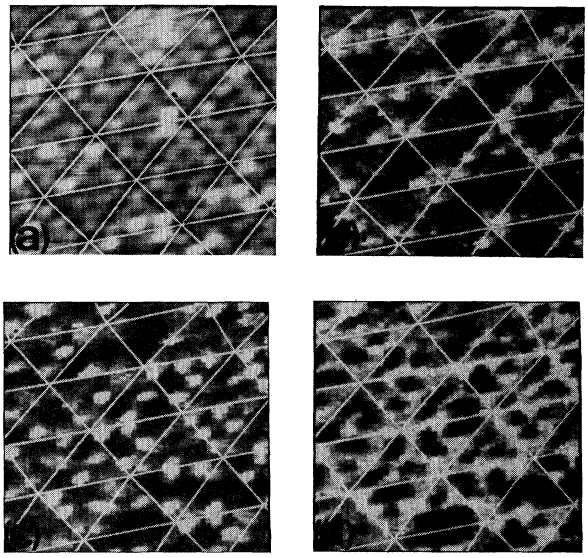

FIG. 4. (a) STM image at a sample bias of -2.5 V, $I=0.5$ nA of a 7×7 reconstruction area of 5×6 nm^2 without drift correction, on which the spectra shown in Figs. 5(a) and 5(b) are taken. The 7×7 net is indicated for comparison with (b)–(d). (b) A current image at -1.0-V sample bias as derived from the spatially resolved I-V curves. The value of the current at this bias is keyed to the brightness of the image. The filled states contributing to this current are localized at about 50% of the adatoms, 60% of which are in the faulted half of the unit cell, and preferentially at corner sites. (c) The current image at $+0.5$-V sample bias. On clean Si(111) 7×7 the state contributing to the current at this voltage is the empty adatom dangling-bond state. In the present case only a fraction of the adatoms exhibit this state. (d) A differential current image showing the increase in current from $+1.5$- to $+2.0$-V sample bias. The bright triangular regions are similar in geometrical appearance as the back-bond states on clean Si(111) 7×7. The adatoms and rest atoms which image bright in the topography are absent in this image.

be demonstrated below that triplets do exist at higher coverages and form a distinct triangular image.

Within the $\frac{1}{3}$-ML $\sqrt{3}\times\sqrt{3}$ reconstructed area imaged in Fig. 2(a), antiphase boundaries can be distinguished. One such boundary is indicated by the dashed line between the arrowheads. The phase shift over these boundaries is precisely $\frac{1}{2}[110]$ pointing from one $T4$ site to another $T4$ site; the bonding site is always $T4$. At the antiphase boundaries, a row of rest atoms with unsaturated dangling bonds remains. There is no evidence for a remaining stacking fault in the second layer.

The LEED study[6] showed $5\sqrt{3}\times5\sqrt{3}$ and $7\sqrt{3}\times7\sqrt{3}$ diffraction patterns. It is tempting to speculate from Fig. 2(a) that these periodicities might arise from an ordering of the dark lines that are present in this figure. The distance between these lines is indeed about 5 to 7 $\sqrt{3}\times\sqrt{3}$ cells.

Figure 3 shows a disorderly looking phase, which we denote "disordered 7×7." A two-dimensional (2D) Fourier transform of the image exhibits the symmetry and periodicity of the 7×7 reconstruction, but the real-space structure is highly disordered. Two 7×7 cells are indicated in Fig. 3, and we observe that most of the unfaulted halves of the unit cells (lower-left halves) are intact, but the adatoms in the faulted half are randomly positioned at $T4$ sites. Corner holes are still clearly observable. A fraction of these show a protrusion in the center.

In the Sb-induced surface reconstructions observed in this study at coverages up to $\frac{1}{3}$ ML, Sb atoms sit on $T4$ sites in order to eliminate three Si dangling bonds each. Possibly, Sb also substitutes Si atoms at rest-atom positions in the 7×7 reconstruction as indicated by STS and discussed below.

2. *Scanning tunneling spectroscopy*

In order to obtain insight into the electronic structure of the Si(111) surface covered with about 0.3 ML of Sb, STS measurements are performed. At 50 positions per scan line, the tunneling current is measured at 100 voltages in the range from −2.5 to +2.5 V, while the tip is kept at a constant distance from the surface.

Figures 4(a) and 5(a) show the topographic image of a 7×7 reconstructed area taken at −2.5-V sample bias and the corresponding average I-V curve taken on this area, respectively. The normalized derivative of the I-V curve $[(dI/dV)/(I/V)]$ is also plotted and shows a peak at +0.3 eV. In comparison to the I-V spectrum on clean Si(111) 7×7, the present spectrum appears rather structureless. On clean Si(111) 7×7, peaks appear at −1.7, −0.8, and −0.3 eV arising from backbond, rest-atom, and adatom dangling-bond states, respectively, as has been demonstrated previously with STS.[19] In the topography, not only the adatoms, but also a fraction of the rest atoms are clearly visible. We speculate that the rest atoms or a fraction of these are substituted by Sb atoms. Si rest atoms have a filled p-like dangling bond and are therefore charged. It seems likely that Sb at that position would be energetically more favorable; it would also have a p-like lone-pair orbital, but would stay neutral. If the lone-pair state has an energy close to the tunneling voltage −2.5 V, it would explain the visibility of the rest atoms in the topography and also the absence of the rest-atom dangling-bond peak at −0.8 eV in the tunneling spectrum.

The current images shown in Figs. 4(b)–4(d) are derived from spatially resolved I-V measurements. The filled states between −1.0 and 0 eV, as shown in Fig. 4(b), are localized at 50% of the adatoms, 60% of which are in the faulted half of the unit cell and preferentially at corner sites.

Figure 4(c) depicts an image of the tunneling current at +0.5 V. On clean Si(111) 7×7, the only state contributing to this current is observed at the adatoms and interpreted as the empty part of a metallic dangling-bond state. Here we find this state at only about 50% of the adatoms, 70% of which are in the unfaulted half of the unit cell. In particular, the adatoms which image brightly in the topograph do not exhibit this state. For Sb adatoms this metallic dangling-bond state is not expected, as for this group-V element a filled lone-pair orbital is present. We conclude that also at the present coverage the adatoms which are brightly imaged in the topograph

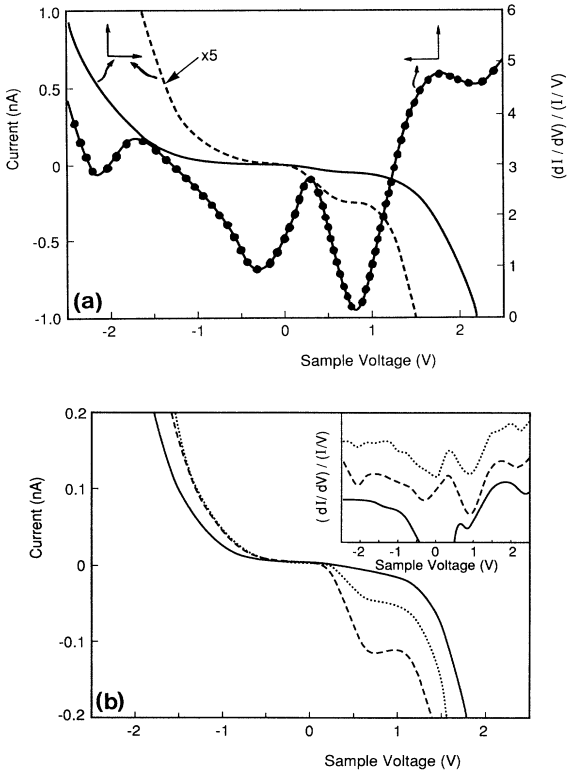

FIG. 5. (a) Average I-V curve taken on the area in Fig. 4(a) and the normalized derivative $(dI/dV)/(I/V)$ tunneling spectrum showing a pronounced peak at +0.3 eV and a rather featureless curve at other energies. (b) Spatially resolved tunneling spectroscopy at various adatom positions. Shown are the spectra over adatoms imaging brightly in the topograph (solid curves), over adatoms imaging brightly in the current image at +0.5 V in Fig. 4(c) (dashed curves), and those showing up in Fig. 4(b) as well as Fig. 4(c) (dotted curves).

are Sb atoms. Remarkably, also some of the dimly imaged adatoms lack the empty dangling-bond state. Therefore, in addition to the clear difference between adatoms, as apparent in the topograph, more subtle differences exist and adatoms imaging similarly at -2.5 V are not necessarily equivalent.

A map of the tunneling current between $+1.5$ and $+2.0$ V is shown in Fig. 4(d). The regions of high tunneling current form triangularly shaped regions similar to the backbond states as reported by Hamers, Tromp, and Demuth.[19] Further noticeable features are the missing adatoms and rest atoms. Again, particularly those adatoms and rest atoms imaged brightly in the topograph are missing.

Figure 5(b) shows spatially resolved I-V curves taken at different adatom sites. There are large differences between the curves. Above bright adatoms almost no tunneling current can be detected between -0.5 and $+0.5$ V as a result of the low DOS there. Conversely, at other adatom positions the current is large near the Fermi level. Also, sites with intermediate behavior are observed. Some adatoms show a strong empty dangling-bond peak, others a strong filled dangling-bond peak. These large variations in the I-V curves are probably caused by the random nature of the Sb substitution of Si atoms. At the present Sb coverage of about 0.3 ML, the local configuration of the adatoms varies in Sb content, leading to a varying electronic structure and the spread in I-V characteristics. Averaging over all positions then leads to the rather featureless spectrum of Fig. 5(a).

B. 1-ML coverage

The surface as depicted in Figs. 6(a)–6(c) is prepared by deposition of about 1 ML of Sb at room temperature and a subsequent anneal of 5 min at 900 ± 50 K, followed by quenching to room temperature. According to the LEED study of Park *et al.*,[6] a phase with a sharp $\sqrt{3}\times\sqrt{3}$ pattern and a phase with diffuse 2×2 (or three-domain 2×1) pattern and a high background coexist at these conditions. The real-space surface as we observe by STM consists of three domains of a 2×1 reconstruction [giving the 2×2 pattern in LEED (Ref. 5)], constituting about 80% of the surface, and patches with a triangular or hexagonal shape, which are slightly elevated.

In Fig. 6(a) an overview of the surface is given, while in Fig. 6(b) various domains of 2×1 are shown. Figure 6(c) shows the reconstructions in atomic detail.

In Fig. 7(a) a schematic representation of our proposed model for the 2×1 structure is shown. Sb atoms are placed on top of the dangling bonds of the truncated Si lattice, leaving two unsaturated p-type orbitals per Sb atom. Neighboring Sb atoms form bonds by moving inward with respect to the axis of the resulting chain. The bond angles are close to 90°, similar to the Sb crystal structure.

The chains run in three $\langle 1\bar{1}0\rangle$ directions, reflecting the threefold symmetry of the underlying lattice. The Sb atoms are relaxed inward with a component in the (111) plane of 0.45 ± 0.15 Å, resulting in a nearest-neighbor distance of 3.1 ± 0.2 Å, as compared to 2.91 Å in the metal. A possible relaxation of the Sb atom positions in the 2×1 reconstruction, parallel to [111], cannot be measured directly. Single 2×1 domains never extend over large areas of the sample, presumably as a result of the accumulating strain. The chains are often terminated by an adatom at a $T4$ site.

In addition to the 2×1 reconstruction, small assemblies of 1×1 structure are observed. Figure 6(c) shows one such assembly in atomic detail. These areas are often composed of triangular subunits separated by a boundary. These compositions of 1×1 structure are elevated with respect to the 2×1 reconstructed part of the surface by 1.3 ± 0.1 Å. The elevation suggests a double-layer structure for the 1×1 areas. A plausible structure is a first layer of Si atoms on lattice sites, with a second layer of Sb atoms on top, on either lattice sites or possibly on sites forming a fault in the stacking sequence. The extra Si atoms needed to form this double-layer structure can be accounted for by the Si adatoms in the original 7×7 reconstruction (about 25% of a ML). A substantial strain will be present in this structure, since the Sb atom is about 20% larger than Si. The 1×1 distance as measured from the STM image is 0.44 ± 0.02 nm [$a=0.384$ nm for Si(111)], and the strain is therefore $(15\pm5)\%$, in agreement with the expected value. The triangular subunits reach maximum dimensions of only five atoms at the side, probably as a result of the accumulating strain. The atomic positions in adjacent triangles appear to be translated with respect to each other by approximately $\frac{1}{6}\langle 11\bar{2}\rangle$. Furthermore, the outermost row of atoms, on the edge of the elevated structure, is laterally on the same lattice as the other top-layer atoms, but is depressed by about 1 Å. These rows forming a $\langle \bar{1}\,\bar{1}2\rangle$ edge (the normal to the edge pointing outward in the $\langle \bar{1}\,\bar{1}2\rangle$ directions) are depressed slightly deeper than the rows forming $\langle \bar{1}\,\bar{1}2\rangle$ edges.

We propose a model which explains these observations and is shown schematically in Fig. 7(b). The first layer of atoms is positioned on the expected lattice sites. The second layer is formed by triangular regions of Sb atoms in a 1×1 structure: triangles with normals to the edges pointing outward to $\langle \bar{1}\,\bar{1}2\rangle$ have the Sb atoms at positions producing a stacking fault and will be called faulted. Those triangles having edge normals toward $\langle 11\bar{2}\rangle$ have the Sb atoms at lattice sites. The domain walls between faulted and unfaulted regions cannot be observed directly with STM, but are presumably similar to the domain walls in the dimer-adatom-stacking-fault model for the 7×7 reconstruction, in which first-layer Si atoms dimerize, to reduce the number of dangling bonds.

In the proposed dimer-stacking-fault (DS) model, the Sb atoms forming the depressed edge rows are bonded to two first-layer Si atoms and to one second-layer Si lattice atom and are therefore depressed. The observed difference in depression of the edge rows is explained naturally by this model: The rows in the faulted half will be repelled by the atoms in the underlying lattices, whereas the rows over hollow sites can move down unhindered.

Another observation in Fig. 6(c) is the presence of isolated trimers that are interpreted as "milk stools" of three Sb atoms, as have been proposed to constitute the

1-ML $\sqrt{3}\times\sqrt{3}$ Si(111)-Sb reconstruction.[16] Mårtensson *et al.* have recently reported a study dedicated to this 1-ML $\sqrt{3}\times\sqrt{3}$ reconstruction.[17] The orientation of the trimers justifies the location over $H3$ sites [see Fig. 7(c)]. Each Sb atom in the trimer has one p-type bond to the substrate Si and two within the trimer. It should be noted that a trimer can easily be discriminated from a single atom image, strengthening the interpretation of the $\frac{1}{3}$-ML $\sqrt{3}\times\sqrt{3}$ image spots as single adatoms.

IV. CONCLUSION

We studied the Sb-induced surface reconstructions on Si(111) at coverages ranging from a few percent of a ML to the saturation coverage of about 1 ML. At a coverage

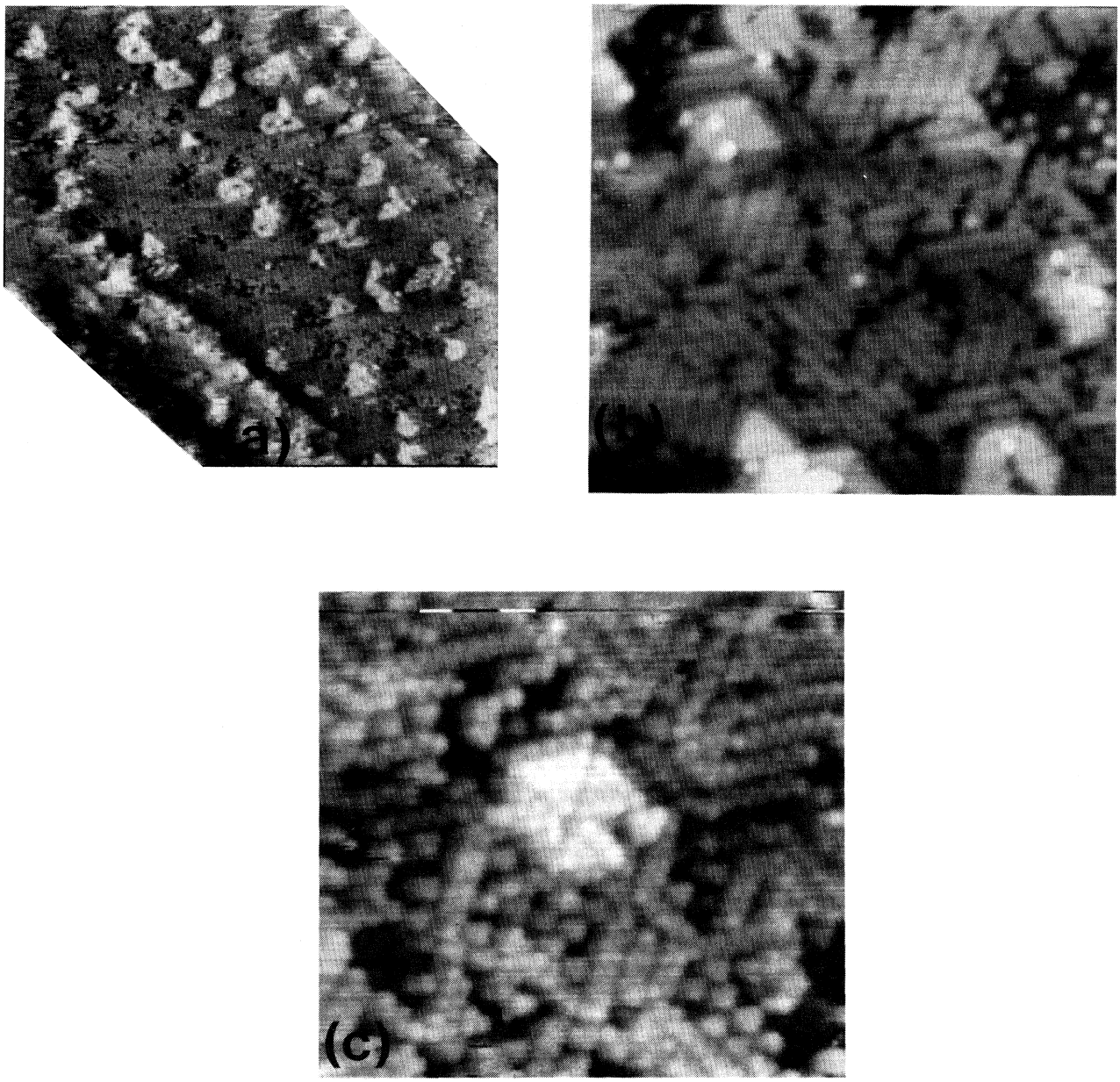

FIG. 6. (a) Si(111) saturated with about 1 ML of Sb deposited at room temperature and annealed for 5 min at 900 K. STM image, 70×70 nm^2, -2.5 V, and 0.5 nA. A (111) terrace is seen between two step bunches (upper right and lower left). The overview shows the existence of a flat terrace with hexagonal and triangular elevated islands. (b) Same surface as in (a) zoomed in to 20×20 nm^2. Domains of the 2×1 reconstruction can be seen oriented in three $\langle 110\rangle$ directions. The structure of the apparent rows is resolved in (c). (c) Same surface zoomed to 12×12 nm^2. Zigzag chains making up the 2×1 reconstruction are resolved in the upper-right-hand corner. In the center an imperfect hexagonal island is shown with local 1×1 structure. Below this island some barely resolved triangularly shaped triplets are imaged. Our proposed structure models are shown in Fig. 7.

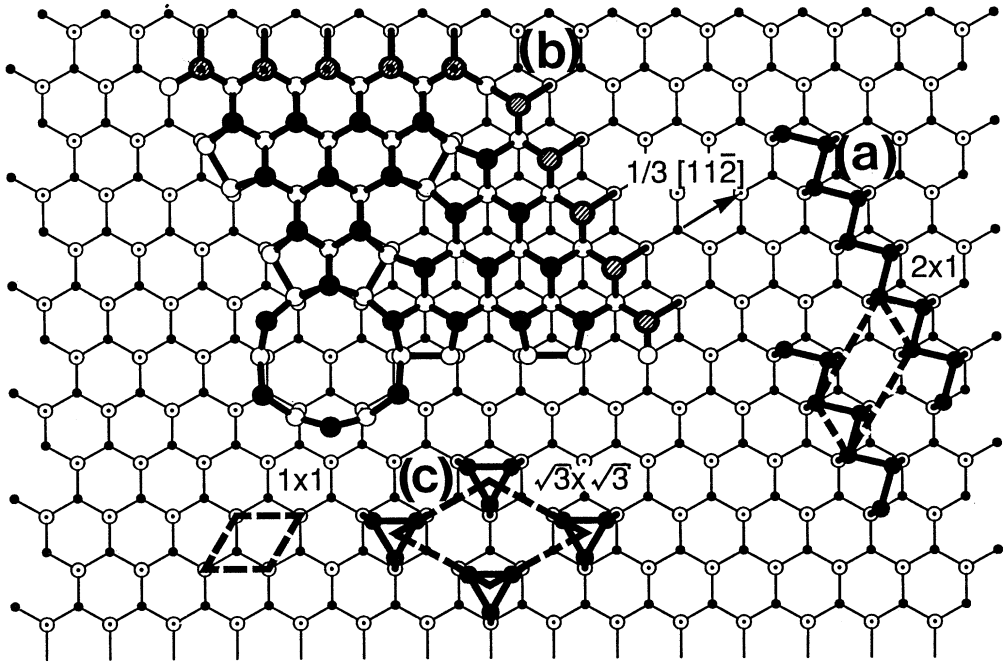

FIG. 7. Structure models for the observed structural features in Figs. 6(a)–6(c). The proposed models are superimposed on the 1×1 Si(111) lattice. One 1×1 cell is indicated by the dashed rhombus. (a) Zigzag chain model for the 2×1 reconstruction. Sb atoms (solid symbols) sit on $T1$ sites and form mutual bonds (solid lines). The 2×1 cell is indicated by the dashed line. (b) Structure model for the observed hexagonal or triangular islands. Open symbols denote first-layer Si atoms, solid symbols are second-layer Sb atoms, and dashed symbols are depressed rows of Sb atoms; see text for a complete description. (c) Milk-stool model for the 1-ML $\sqrt{3}\times\sqrt{3}$ reconstruction.

below $\frac{1}{3}$ ML, Sb atoms are located on $T4$ adatom sites either by substituting Si adatoms randomly with a preference for the faulted half of the 7×7 reconstruction or by inducing the $\sqrt{3}\times\sqrt{3}$ adatom reconstruction. Also, we found indications that Si atoms at rest-atom sites in the 7×7 reconstruction may be substituted by Sb. In all these substitutions, the energetically unfavorable unsaturated dangling bond of the substituted Si atom is replaced by a lone-pair orbital of the Sb atom. Sb is found to adsorb preferentially in the faulted half of the 7×7 unit cell.

Spatially resolved STS showed the complexity of the electronic structure of the Si(111) 7×7 Sb surface, as compared to the clean Si(111) 7×7 surface. The random nature of the substitution of Si atoms by Sb leads to a vast variation in electronic structure, even at similar locations in the unit cell.

At 1-ML coverage we observed the 1×1, 2×1, and $\sqrt{3}\times\sqrt{3}$ phases of Si(111)-Sb simultaneously, and we propose structure models for these reconstructions. In all of these reconstructions, the surface is passivated by the elimination of all unsaturated dangling bonds, which explains the Sb saturation of the surface near 1-ML coverage.

ACKNOWLEDGMENTS

The support of Dr. J. Dieleman is gratefully acknowledged, and we thank Mark Venbrux for his continuous efforts in improving the data-analysis software and his fast responses to our requests.

[1]M. Copel, M. C. Reuter, E. Kaxiras, and R. M. Tromp, Phys. Rev. Lett. **63**, 632 (1989).
[2]M. A. Olstead, R. D. Bringans, R. I. G. Uhrberg, and R. Z. Bachrach, Phys. Rev. B **35**, 3945 (1987).
[3]R. S. Becker, B. S. Swartzentruber, J. S. Vickers, M. S. Hybertsen, and S. G. Louie, Phys. Rev. Lett. **60**, 116 (1988).
[4]M. Copel, R. M. Tromp, and U. K. Köhler, Phys. Rev. B **37**, 10 756 (1988).
[5]J. R. Patel, J. Zegenhagen, P. E. Freeland, M. S. Hybertsen, J. A. Golovchenko, and D. M. Chen, J. Vac. Sci. Technol. B **7**, 894 (1989).
[6]C. Y. Park, T. Abukawa, T. Kinoshita, Y. Enta, and S. Kono, Jpn. J. Appl. Phys. **27**, 147 (1988).
[7]J. Stroscio, R. Feenstra, and A. P. Fein, Phys. Rev. Lett. **58**, 1668 (1987).
[8]J. Nogami, Sang-il Park, and C. F. Quate, Surf. Sci. Lett. **203**,

L631 (1988).
[9]J. Nogami, Sang-il Park, and C. F. Quate, J. Vac. Sci. Technol. B **6**, 1479 (1988).
[10]J. Nogami, Sang-il Park, and C. F. Quate, J. Vac. Sci. Technol. A **7**, 1919 (1989).
[11]St. Tosch and H. Neddermeyer, Surf. Sci. **211/212**, 133 (1989).
[12]U. Koehler, J. E. Demuth, and R. J. Hamers, Phys. Rev. Lett. **60**, 2499 (1988).
[13]K. M. Conway, J. E. MacDonald, C. Norris, E. Vleig, and J. F. Van Der Veen, Surf. Sci. **215**, 555 (1989).
[14]A. Kawazu and H. Sakama, Phys. Rev. B **37**, 2704 (1988).
[15]R. J. Hamers, Phys. Rev. B **40**, 1657 (1989).
[16]T. Abukawa, C. Y. Park, and S. Kono, Surf. Sci. **201**, L513 (1988).
[17]P. Mårtensson, G. Meyer, N. M. Amer, E. Kaxiras, and K. C. Pandey, Phys. Rev. B **42**, 7230 (1990).
[18]C. Y. Park, T. Abukawa, K. Higashiyama, and S. Kono, Jpn. J. Appl. Phys. **26**, L1335 (1987).
[19]R. J. Hamers, R. M. Tromp, and J. E. Demuth, Phys. Rev. Lett. **56**, 1972 (1986).

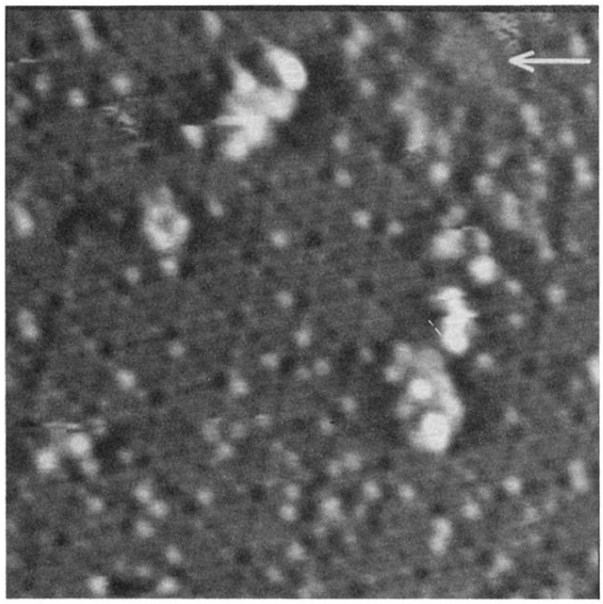

FIG. 1. STM image of 24×20-nm^2 Si(111) 7×7 area after deposition of about 0.03 ML of Sb and an anneal of 2 min at 900 ± 50 K. $V_{\text{sample}}=-2.5$ V, $I=0.5$ nA. Brightly imaged adatoms and clusters and a nucleus of the $\sqrt{3}\times\sqrt{3}$ reconstruction (arrow) can be seen.

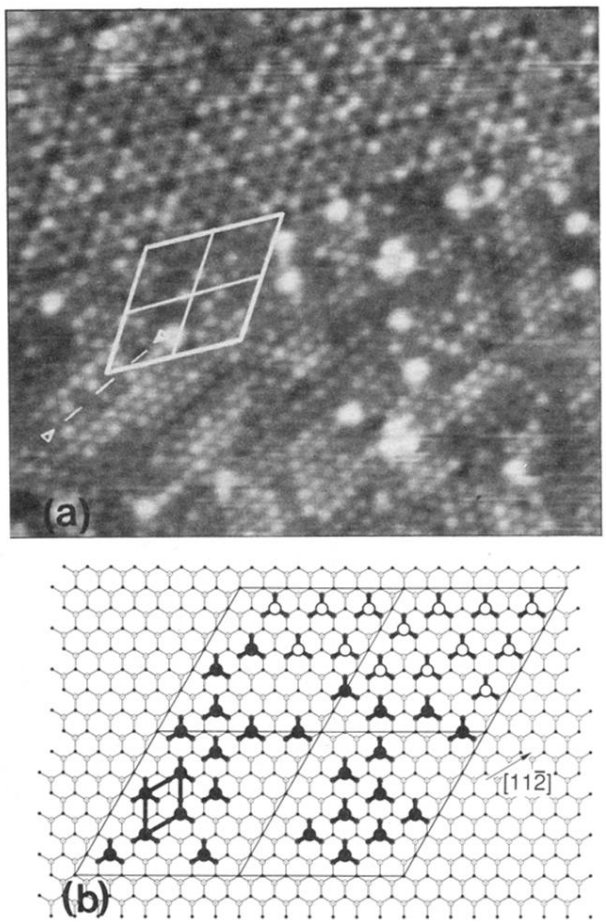

FIG. 2. (a) STM image of 25×22-nm^2 Si(111) surface with about 0.3 ML of Sb, after 2-min anneal at 1000 ± 50 K. $V_{\text{sample}}=-2.5$ V, $I=0.5$ nA. A phase boundary between the 7×7 and $\frac{1}{3}$-ML $\sqrt{3}\times\sqrt{3}$ reconstruction is observed. The area in the rhombus is mapped in (b). The dashed line between the arrows indicates an antiphase boundary within the $\sqrt{3}\times\sqrt{3}$ area. (b) Schematic representation of the adatom positions in the 7×7 and $\frac{1}{3}$-ML $\sqrt{3}\times\sqrt{3}$ reconstructions as seen in (a); a $\sqrt{3}\times\sqrt{3}$ cell is indicated. Open symbols denote adatoms in the 7×7 reconstruction; solid symbols denote adatoms in the $\sqrt{3}\times\sqrt{3}$ reconstruction. All adatoms are located on $T4$ sites. Stacking faults and dimers which are present in the 7×7 reconstruction are omitted.

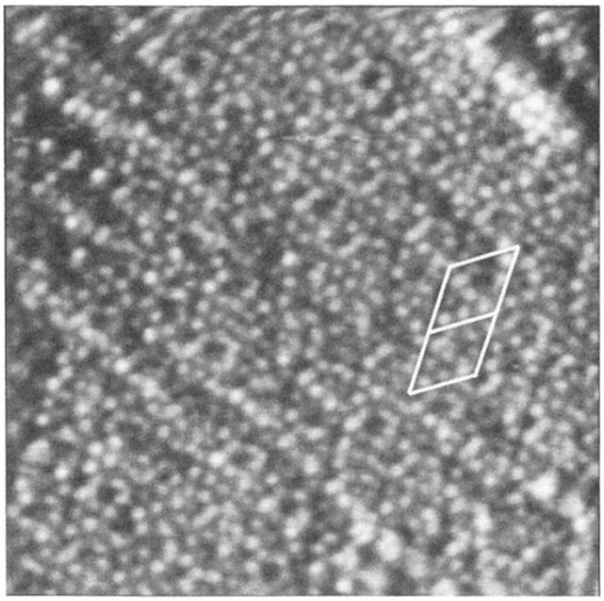

FIG. 3. STM image at a sample bias of -2.5 V, $I=0.5$ nA, and 24×24 nm^2. A 2D fast Fourier transform shows the 7×7 periodicity, but the real-space structure is highly disordered. Two 7×7 cells are indicated. Corner holes are recognizable and often contain a protrusion in the center. The adatoms in the faulted half (upper-right half) of the unit cells are located on random $T4$ sites, while in the unfaulted half most are at the correct position in the 7×7 reconstruction.

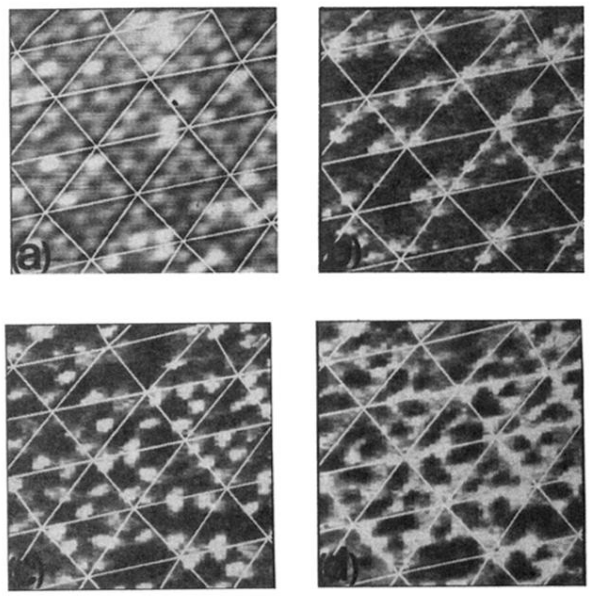

FIG. 4. (a) STM image at a sample bias of -2.5 V, $I=0.5$ nA of a 7×7 reconstruction area of 5×6 nm^2 without drift correction, on which the spectra shown in Figs. 5(a) and 5(b) are taken. The 7×7 net is indicated for comparison with (b)–(d). (b) A current image at -1.0-V sample bias as derived from the spatially resolved I-V curves. The value of the current at this bias is keyed to the brightness of the image. The filled states contributing to this current are localized at about 50% of the adatoms, 60% of which are in the faulted half of the unit cell, and preferentially at corner sites. (c) The current image at $+0.5$-V sample bias. On clean Si(111) 7×7 the state contributing to the current at this voltage is the empty adatom dangling-bond state. In the present case only a fraction of the adatoms exhibit this state. (d) A differential current image showing the increase in current from $+1.5$- to $+2.0$-V sample bias. The bright triangular regions are similar in geometrical appearance as the back-bond states on clean Si(111) 7×7. The adatoms and rest atoms which image bright in the topography are absent in this image.

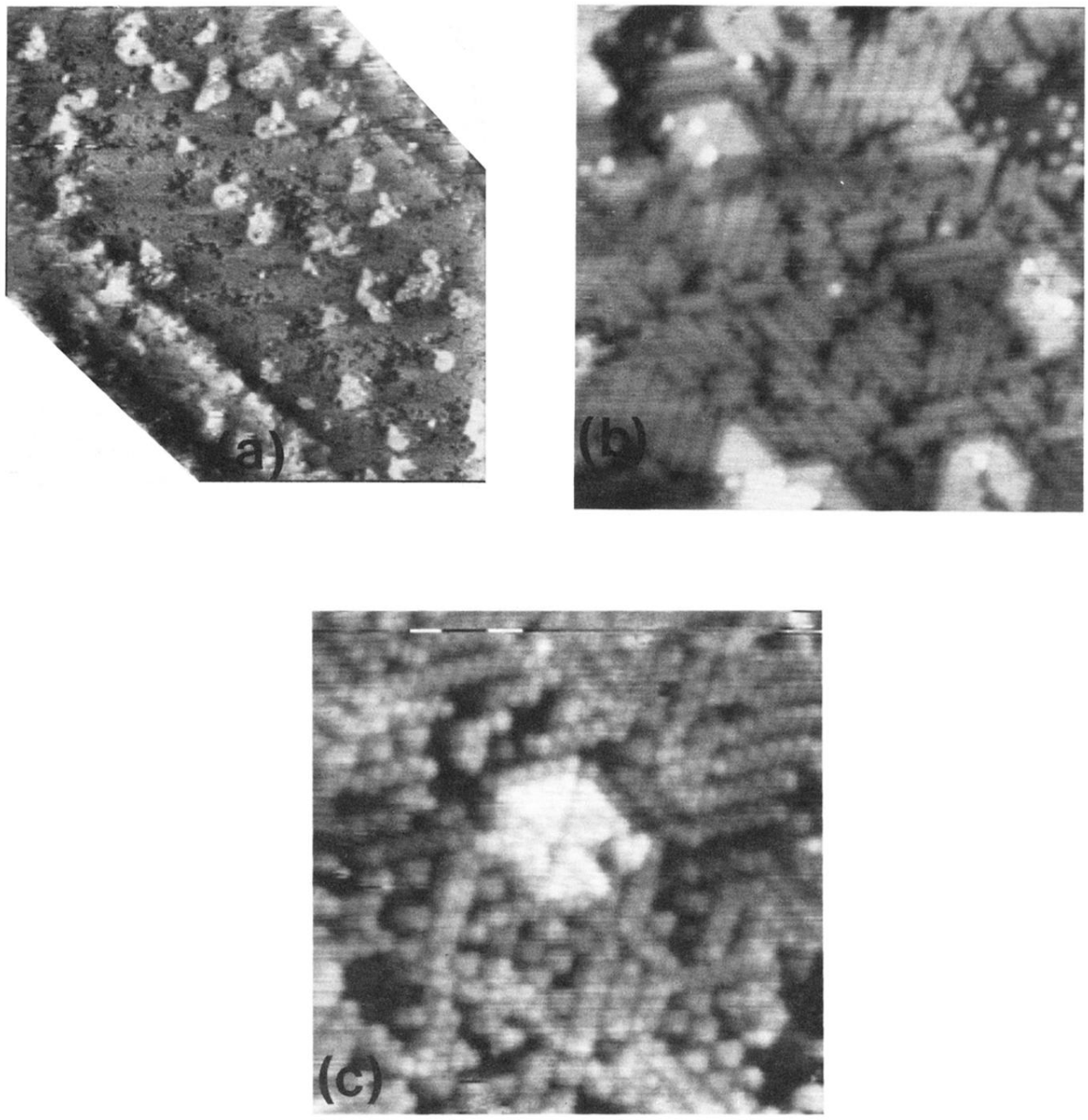

FIG. 6. (a) Si(111) saturated with about 1 ML of Sb deposited at room temperature and annealed for 5 min at 900 K. STM image, 70×70 nm^2, -2.5 V, and 0.5 nA. A (111) terrace is seen between two step bunches (upper right and lower left). The overview shows the existence of a flat terrace with hexagonal and triangular elevated islands. (b) Same surface as in (a) zoomed in to 20×20 nm^2. Domains of the 2×1 reconstruction can be seen oriented in three $\langle 110 \rangle$ directions. The structure of the apparent rows is resolved in (c). (c) Same surface zoomed to 12×12 nm^2. Zigzag chains making up the 2×1 reconstruction are resolved in the upper-right-hand corner. In the center an imperfect hexagonal island is shown with local 1×1 structure. Below this island some barely resolved triangularly shaped triplets are imaged. Our proposed structure models are shown in Fig. 7.